SCALE PREDOMINANCE DIAGRAMS FOR BAYER PRECIPITATION TANKS

Gillespie A[1,2*], Hawker W[1], Jayawardana V[1], Hayes P[1]

[1] *School of Chemical Engineering, The University of Queensland, Brisbane, Queensland, Australia*
[2] *Rio Tinto Alcan – QRDC, Queensland, Australia*

Abstract

Scale formation in Bayer precipitation tanks constrains slurry flow, reduces tank volume and adds mechanical stress to tanks and associated process equipment. Combined, these factors decrease precipitation productivity and increase the levels of process and safety risk. The Australian alumina industry therefore considers scale management generally, and precipitation scale formation specifically, to be critical areas of research and development over the next 15 -20 years.

In plants that practice sodium oxalate co-precipitation as a means of organics removal, there are often dramatic differences in scaling rate, scale structure and scale distribution between adjacent tanks. The objectives of this project were to explain such differences and to provide detailed mechanistic models that will allow existing processes to be optimised and/or other scale reduction technologies to be successfully applied.

In the Bayer precipitation and classification circuit, crystallisation fouling, particulate fouling and erosion processes were found to compete to determine the type and extent of scale formation. By conducting detailed analyses of scale samples obtained from an alumina refinery, and of those prepared under controlled conditions in the laboratory, the key factors in each of these processes were determined.

This paper describes the simulation of fouling in a laboratory crystalliser, provides supporting measurements of local slurry velocity and flow patterns in an equivalent physical model, and introduces the concept of the *scaling predominance diagram*. The scaling predominance diagram, when accurately mapped, provides an important means of quantifying the opportunities to change the scaling regimes in Bayer precipitation tanks and other key parts of the process plant.

1. Introduction and literature review

The majority of the aqueous solutions employed within the Bayer process are supersaturated with respect to at least one solid phase. As a direct consequence there is a natural tendency for solid phases to form, either as discrete particles that remain suspended in the slurry, or as scale on the walls and surfaces of process equipment. Scale is an undesirable product because it constrains slurry flow, reduces tank volume and adds mechanical stress, thereby contributing directly to reducing plant productivity and increasing production cost (Roadmap 2006, 2010). The project described in this paper is focussed specifically on precipitation tank scale, with the aim of developing improved mechanistic models of the processes that lead to scale formation. For the sponsor company a particular aim was to understand why some adjacent tanks, with apparently similar process conditions, develop dramatically different types of scale. More broadly the aim was to develop a general methodology that can be readily used and applied to the study and analysis of scale formation in reactive systems in a range of well-defined process conditions.

Despite the high cost of precipitator scale formation, the literature reports few studies that make direct reference to precipitator scale. There is, however, a considerable body of knowledge related to crystal and particle formation processes in Bayer slurry and to analogous fouling processes in other systems. Fouling is defined as *the accumulation of undesired solid material at phase interfaces*, and is usually classified on the basis of the key physical/chemical processes through which the *foulant* accumulates (Epstein 1983). In *crystallisation fouling*, dissolved molecules or ions form solids by directly precipitating or crystallising onto surfaces from solution (Bott 1997, Taborek 1972). In *particulate fouling,* suspended particles accumulate on surfaces (Kuppan 2000). In *corrosion fouling*, metal surfaces react to form corrosion products that are retained on the surface. In *reaction fouling* organic reactions, such as, polymerization, cracking and coking of hydrocarbons result in insoluble products (Watkinson 1997). In *biological fouling*, adsorbed nutrients attract bacteria that then grow into biological films on surfaces (Characklis 1990). In *solidification fouling*, liquid, or the higher-melting constituents of a multi component solution, freezes on a heat transfer surface.

In the Bayer process, the terms *growth scale* and *settling-cementation scale* (Roach 1985, 1994, 1996) describe *crystallisation fouling* and *particulate fouling* processes respectively. The open literature does not report reaction fouling, biological fouling or solidification fouling in Bayer precipitation tanks. Corrosion fouling is not specifically reported for Bayer precipitation tanks, although the corrosion of associated pipes and vessels is widely reported (Rihan 2006).

The rate at which scale deposits form has been described in terms of the net difference between instantaneous rates of the relevant scale deposition and removal processes (Kern 1959, Muller-Steinhagen). When examined in detail, the following sequence of sub-processes is found to occur. (1) Initiation – or *delay, nucleation, induction, incubation, surface conditioning* - is associated with the delay period that is often observed before fouling becomes apparent. In inorganic systems initiation is generally associated with nucleation, and tends to decrease with increasing temperature, supersaturation and surface roughness. (2) Transport - or *mass transfer* – is the movement of the fouling species from the bulk fluid to the surface, by diffusive or convective forces. The fouling species may be solute or colloidal or macroscopic particles. (3) Attachment – or *surface integration, sticking, adhesion, bonding* – results from liquid-solid phase transformation (i.e. of dissolved ions or molecules) at the surface, or incorporation of suspended particles into the fouling deposit. (4) Removal – or *release, re-entrainment, detachment, scouring, erosion, spalling, sloughing off, shedding* – occurs when the local shear rate is sufficient to remove the fouling deposit. (5) Ageing may cause the chemical or crystalline composition of the deposit to change, and may result in it becoming stronger or weaker.

Gibbsite scale initiation has been investigated by a number of researchers . Pearson *et al* suspended steel samples in Bayer liquor and then measured the scale microstructure (Pearson 2008). After one hour exposure, no changes in surface microstructure were apparent. After two hours, extensive nucleation and crystal growth had occurred and the resulting discrete crystals had grown to 2 - 5 mm in size. After four hours the steel surface was almost completely covered with a polycrystalline gibbsite layer of 2 - 10 mm in thickness. By twenty four hours all of the surfaces were covered with continuous layer of scale. Using surface chemical analysis methods Loan et al measured the relative amounts of surface and sub-surface aluminium, oxygen and iron compounds, on mild steel that had been exposed to laminar-flowing Bayer liquor (Loan 2008). In that investigation a 0.4 nm-thick layer of aluminium tri-hydroxide was found to form rapidly on top of a pre-existing magnetite surface layer. After forming the $Al(OH)_3$ layer, no change was observed in surface chemical composition until after 60 minutes had elapsed, at which time small, discrete gibbsite crystals were observed.

Breault and Bouchard noted that by modifying the steel surface so that a gibbsite layer cannot form, further gibbsite nucleation and crystallisation was prevented (Breault 2008). Their chosen method of surface modification was electrochemical; by applying a cathodic potential the steel surface was maintained in the immunity region, in which state it did not offer a suitable bonding environment for gibbsite. Breault and Bouchard speculated that in the immunity region, the key factor in preventing scale formation was the absence of surface hydroxyl groups, which provide a suitable substrate for gibbsite to bond. An alternative electrochemical method was reported by Scadan and Laurila, who proposed the imposition of anodic surface potential to control scale formation (Scadan 2008). Instead of using electrochemical passivation, Pearson *et al* proposed the use of polymer coatings that adhere to the steel surface and present a non-adhesive surface to the scale (Pearson 2008).

Transport of reactant has been studied in detail for many systems. In crystallisation, corrosion, reaction or solidification fouling, the reactant species is an ionic or molecular entity, whereas in particulate or biological fouling it is colloidal or particulate. For molecules or small particles undergoing Brownian diffusion in laminar flow, the relevant transport equations may be solved analytically for some equipment geometries. In turbulent flow, for which analytical solutions of the transport equations are not usually possible, the mass deposition rate of colloidal or particulate material may instead be represented in terms of dimensionless *deposition velocity* and *particle relaxation time* parameters (Papavergos 1984). Three regimes of particle transport in turbulent streams have been noted. In the *diffusional deposition* regime, particles follow the fluid motion in turbulent eddies. In the *diffusion-impaction* regime particles tends to deviate from that of fluid near a wall as a result of inertial force. In the *inertia-moderated* regime, the inertia induced motion of particles tends to prevail over the entire region of the fluid.

A key particle transport mechanism in the diffusion-impaction regime is reportedly *turbophoresis*, a process in which particles are transported along the gradient of the fluctuating component of the fluid velocity in the direction normal to a wall (Deev 2009). Rasheed measured near-wall fluid velocities in pipes by the particle image velocimetry (PIV) technique under fluid dynamic conditions that simulated a slurry transport pipe in an alumina refinery, and found the fluctuating normal-to-wall component was elevated within a so-called *concentric reducer* pipe union (Rasheed, 2005). This finding was consistent with reported particulate fouling patterns in alumina refinery slurry pipes associated with precipitation tanks (Nawrath 2006).

Scale removal – i.e. by release, re-entrainment, detachment, scouring, erosion, spalling, sloughing off or shedding of scale - was indirectly examined by Wu *et al* who reported fluid dynamic and physical modelling investigations of so-called *Swirl Flow Technology* (SFT) precipitation tanks (Wu 2011). A key advantage of SFT was reportedly the doubling of the service life between de-scaling operations. Wu *et al* noted that slurry velocity near to the tank wall, immediately adjacent to the boundary layer, is a key determinant of scale suppression. On the basis of measured and model data, the primary conclusion was that SFT induces near-wall fluid velocity some four times greater than in conventional draft-tube agitated tanks. It was not reported whether, in order to achieve complete slurry suspension, such high near-wall velocity exceeded the threshold for scale formation by a significant margin.

It is evident that previous studies of scale initiation and particle transport apply to smooth, clean model surfaces but don't account for modification of the surface chemistry or topography of the steel surfaces. Further, the published reports imply that variation in transport rate accounts for all of the variation in scale formation rate; no account being taken of the potential for turbulent diffusion to overwhelm turbophoresis, nor of the rate of particle attachment. None of the papers considers Bayer scale formation holistically, i.e. according to the generally accepted initiation-transport-attachment-removal-ageing paradigm. None have examined the factors which determine the predominance of crystallisation, particulate fouling or erosion under specific process conditions Regarding this final point, there is therefore an opportunity to add value by mapping the crystallisation/particulate/erosion fouling *parameter-space,* i.e. the range of conditions under which each of these mechanisms is predominant. This will allow plant operators to select process conditions appropriate for scale management, as well as giving quantitative insight into the scale formation mechanism.

2. Laboratory simulation of scale growth

2.1 Experimental method

Fouling experiments were conducted using a 5L, isothermal, stirred tank crystalliser equipped with in-situ conductivity measurement, concentrated liquor feed and representative slurry removal (Figure 1). The crystalliser was operated in the semi-continuous mode, in which the initial seed material agglomerates, nucleates and grows as a batch, while liquor oxalate and/or alumina levels remain approximately constant (typically for 3-4 days). Steel substrate plates were suspended in the crystalliser, thereby allowing repetitive sampling of the fouled surfaces. Prior to experimentation, the plates were rough polished on both sides (600 grit SiC) then fine polished on a buffing wheel with CrO polishing compound (Dialux Vert™Lippert Unipol). One side of the substrate was then roughened using 90 mm SiC. Prior to insertion in the crystalliser, the plates were cleaned ultrasonically in distilled water to remove excess grinding media.

Start liquor and aluminate feed liquor were prepared by autoclave digestion of laboratory grade sodium hydroxide, sodium carbonate, gibbsite and analytical grade water. These solutions were prepared in concentrated form, with the remaining water set aside for dissolution of sodium oxalate. The concentrated start liquor was mixed with its corresponding oxalate solution immediately prior to the start of the fouling experiment. The concentrated feed liquor, and its corresponding oxalate solution, were mixed in the feed stream to the crystalliser. The crystalliser was operated at 65°C or 74°C, while feed solutions were maintained at room temperature. In the following sections the slurry composition is defined in terms of the caustic level (C, g/L as Na_2CO_3), gibbsite relative supersaturation (s_g), sodium

oxalate relative supersaturation (s_{ox}), start solids loading (f g/L), and temperature (T, °C). Gibbsite solubility was calculated using the correlation of Rosenberg and Healy (Rosenberg 1996); sodium oxalate solubility was calculated using an unpublished correlation provided by the project's sponsor .

For seeded experiments, washed and dried plant gibbsite seed was added. The suspension was agitated by axial flow impeller at various stirring rates. Slurry and substrate samples were obtained periodically (typically twice per day). Substrate samples were immediately rinsed sequentially with cold water, cold ethanol and cold acetone then air-dried at room temperature and mounted on pin-stubs for microscopic analysis. Slurry samples were obtained for liquor ACS analysis by gluconate titration (Connop 1996), liquor oxalate analysis by ion chromatography, and particle size analysis by the single particle optical sensing method (Audet 2005). At the end of some of the experiments the crystalliser was rapidly emptied by suction hose and the scale distribution recorded. While still moist, contiguous sections of scale were removed intact from the tank wall, then air dried for 48 hours. Sub-samples of the dried scale were mounted on pin stubs for microstructural analysis (SEM), and re-slurried in hot water for particle size analysis.

In order to obtain quantitative relationships between scale deposition and local fluid and particle velocities, a physical model of the crystallizer was built. The model was constructed of transparent acrylic and, being within 90% on most dimensions, was dimensionally similar to the laboratory crystalliser. The cone and fillet bottom in the cold model was hand-made of moulding plaster and then waterproofed using a brush-on compound. Agitation was provided by the impeller and drive that were normally fitted to the laboratory crystalliser. The experimentation was carried out using water as the fluid medium, and tracer particles prepared from micro-balloons and casting resin. The tracer particles were ring ground, then dry screened to a nominal size range of -106 µm then float/sink tested to ensure a density range close to that of water.

2.2 Gibbsite crystallisation fouling experiments

In oxalate-free synthetic Bayer liquor (C=220, s_g=0.5-1.1, s_{ox}=0, f=0,2.1,T=65), gibbsite crystallisation was the predominant fouling mechanism. The typical evolution of the scale microstructure on the steel substrate is shown in Figure 2. After 19 hours, randomly distributed, small (~1 mm) independent crystallites were associated with fine scratches on the steel substrate. At 48 hours, significant crystal growth was evident, the crystallites being ~5 mm and of morphology typical of small gibbsite crystals (Sweegers 2001, 2002). At this stage there were no independent crystallites, however crystallite intergrowth was minimal. At 92 hours significant crystal intergrowth was evident, the resulting polycrystalline array of ~9 mm hexagonal-based, square edged prisms demonstrating a high degree of crystal intergrowth. Scale microstructure was strongly influenced by substrate preparation, the roughened substrate having greater particle coverage during the initiation and independent growth phases, and less dendrite growth during the polycrystalline growth phase. The deposits formed on smooth substrates were poorly adhered and, unlike those on the roughened surface, easily delaminated at or near the substrate/scale boundary. For seeded slurries in which gibbsite supersaturation was allowed to drop towards the equilibrium level, there was subsequent evidence of erosion. Erosion did not occur in unseeded slurries, for which the slurry solids loadings were minimal even at extended run times. In seeded slurries there was no visual evidence of particulate fouling of the substrates or of the walls of the crystalliser.

2.3 Gibbsite/oxalate particulate fouling experiments

In synthetic Bayer liquor that was supersaturated in both sodium oxalate and gibbsite (C=218, s_g=0.5-1.1, s_{ox}=0.3-0.7, f=2.1, T=65), particulate fouling was the predominant fouling mechanism. Scale deposits were most clearly observed on the walls and internal components of the crystalliser at the end of the experiments (Figure 3). While still moist, the scale was only weakly bound to the steel surface and was easily removed in flexible sheets. On drying, the scale hardened to form cohesive, strongly adhered deposits that were resistant to removal by scraping. The scale was unevenly distributed in the circumferential, radial (i.e. normal to the surface) and vertical directions on the inner surface of the crystalliser. At high agitation rate (300rpm) scale was formed on the vessel wall between the slurry surface and the top of the draft tube, and there was minimal deposition on the lower walls of the vessel and on the draft tube and baffles. At low agitation rate (50rpm) scale formed on the vessel wall 20 – 30 mm below the level of the top of the draft tube, as well as on the inner walls of the draft tube.

A variety of patterns and topographical features were observed at the microscopic level (Figure 4). Scale obtained from the most heavily fouled experiment was composed of randomly arranged gibbsite particles and sodium oxalate needles. Sodium oxalate was the dominant constituent phase and accounted for approximately 68% of the mass of the sample. Gibbsite particles (polycrystalline agglomerates of shape and microstructure equivalent to those in the seed and slurry) were not regularly dispersed in the scale, regions of high and low gibbsite particle population being separated by only a few millimetres. By dissolving the sodium oxalate in hot water the gibbsite particles were easily separated. The maximum gibbsite particle diameter in the scale was approximately 30 mm, compared with ~74 mm in the seed material and ~90 mm in the final slurry.

2.4 Sodium oxalate crystallisation fouling experiments experiments

In oxalate-supersaturated synthetic Bayer liquor (C=219, s_g=0.1, s_{ox}=0.2, f=2.1, T=65), at slight gibbsite supersaturation and in the presence of gibbsite seed, the crystalliser showed significant fouling (Figure 5). As with most of the fouling experiments at 300 rpm agitation rate, fouling only occurred on regions of the crystallizer wall that were in line with, or above the top of the draft tube. The deposit was less thick than gibbsite-oxalate particulate deposits and mostly comprised of discrete clusters which, in some areas, appeared in the form of circumferential rings. The scale was predominantly compromised of acicular sodium oxalate crystals, sized in the range 0.1 x 1 mm (width x length) to 20 x 200 mm. The finest sodium oxalate crystals were mostly associated with the smallest faces of the largest sodium oxalate crystals. Hexagonal gibbsite platelets smaller than 100 x 500 nm (thickness x width) were observed clustered on the faces of some of the acicular sodium oxalate crystals, however there was no evidence of the polycrystalline gibbsite particles added to the crystalliser. As for gibbsite/oxalate particulate fouling the oxalate needles appeared as porous, low density networks (Figure 6). Many of the coarse oxalate crystals showed interpenetrating growth, suggesting that there had been a significant period of crystallisation to strengthen the deposit.

2.5 Physical modelling of particle and fluid flow

The method chosen for velocity modelling was particle image velocimetry (PIV), a technique based on mapping the position of tracer particles to determine fluid velocity. The particles are assumed to follow fluid streamlines, therefore a comparison of the position of any given tracer particle between frames indicates equivalent fluid movement. PIV comprises three sequential steps: recording the experiment, image processing and evaluation

of velocity vectors. Video based PIV analysis was conducted successfully with compact digital cameras operating with frame rates in the range of 30 – 240 s^{-1}. Experiments were conducted in a darkened room with a black background and particles were illuminated by a combination of halogen light and incandescent lamp. The videos were edited by applying grayscale and contrast filters to ensure errors from reflections were minimised and only fully illuminated tracer particles were visible.

Open-source Matlab® based programs were used to conduct image analysis involving particle position correlation between frames and the generation of velocity vector fields. Filters within the programs removed erroneous vectors and smoothed velocity vectors, with the time interval for particle tracking based on the frame rate. An example of the velocity profiles within the outer shell of the model crystalliser obtained using the optical PIV technique is shown in (Figure 7). The arrows indicate the relative magnitudes and directions of flow for a given impeller rotation rate. These velocity profiles are then used to determine the critical flow conditions for scale formation within the actual crystalliser.

3. Discussion

To quantify the factors that affect the location and rate of particulate scale growth, a conceptual mathematical model was developed. Here the scale growth rate is equal to the so-called fouling velocity, $dz/dtdz/dt$, where *z* is the spatial coordinate normal to the substrate surface. According to the model, the fouling velocity is directly proportional to the net particle flux towards the substrate, i.e.

$$\frac{dz}{dt} = \frac{\left(J_d - J_r\right)}{\xi}$$

where J_d and J_r are the particle volumetric deposition and removal fluxes respectively, and $\xi\xi$ is the void fraction of the resulting deposit. The numerator in Equation 1 is given by

$$J_d - J_r = f\left(\tau_p^+, \phi\right)\left(1-\varphi\right) - k_c c_s n\left(L_{\min}\right)\left(F - F_{\min}\right)$$

where τ_p^+ is the so-called *dimensionless particle deposition velocity* (Papavergos 1984), ϕ is the volume fraction solids in the bulk slurry, φ is the particle sticking probability (i.e. the probability of a transported particle sticking to the deposit), k_c is a rate constant, c_s is the surface concentration of attached particles, $n\left(L_{\min}\right)$ is the concentration of colliding particles with sufficient energy to remove particles, F is the force associated with the specific particle removal process, and $F_{\min}$ is the minimum force required for particle removal. When the second of the above equations is expanded, a number of additional terms and coefficients are added. Some of these may be excluded; for example, buoyancy and fluid drag forces are negligible compared with particle-scale collision forces, hence the former may be excluded from the erosion term. However even when unnecessary terms are excluded the resulting model contains a significant number of coefficients that still must be estimated. Although estimates of the coefficients are possible, tuning the model over a broad parameter range was found to be a highly subjective exercise.

To focus the experimentation on sets of conditions that would yield the most efficient use of the experimental capability, the key variables that determine the conditions under which particulate fouling could predominate over erosion or crystallisation fouling processes were identified. The key variables are: slurry velocity (*v),* fluid turbulence, particulate loading (*f*), particle size (*L*), liquor supersaturation (with respect to gibbsite and sodium oxalate (s_g, s_{ox}). For particulate fouling to dominate, the model predicts a requirement for high slurry solids loading (i.e. high *solids concentration*), fine particle size, low slurry velocity relative to the deposition surface, and high supersaturation. For crystallisation fouling to dominate, there is a requirement for low solids loading, small particle size, low velocity and low supersaturation. For erosion to dominate there is a requirement for high slurry velocity, high solids loading, coarse solids and low supersaturation.

By identifying the relative magnitudes of the processes taking place at the substrate surface it is possible to describe the specific conditions under which various scaling regimes are predominant. In this way *scaling predominance diagrams* can be constructed to describe the behaviour of selected systems. A hypothetical two dimensional scaling predominance diagram is shown in Figure 8. The choice of axes - mean diameter and solids loading respectively – was made from the set of key variables described in the conceptual model. Solid lines, termed *scale boundaries*, define the specific sets of conditions under which there is transition between particulate fouling, crystallisation fouling and erosion regimes. For a given set of operating conditions (i.e. the mean particle size and solids loading of the slurry in that tank) it is possible to identify on the diagram the *operating point* for a single process vessel. The operating point indicates the predominant fouling mechanism for that specific set of operating conditions.

When slurry velocity and supersaturation are changed, the scale boundaries move. Increasing the slurry velocity and/or turbulence may increase the erosion rate as illustrated in Figure 8b; moving from v_1 to v_2 changes the predominant regime from particulate fouling to no fouling. Increasing the liquor supersaturation may increase the cementation rate as illustrated in Figure 8c; moving from $SSAT_1$ to $SSAT_2$ changes the predominant regime from crystallisation fouling, to particulate fouling. On the other hand, when solids loading and/or particle diameter are changed, the *operating point* may shift as shown in Figures 8d. In this example an increase in solids concentration from f_1 to f_2 moves the predominant fouling mechanism from crystallisation to particulate fouling.

The fouling predominance diagram, if accurately constructed, provides a means of quantifying the opportunity to change the predominant fouling regime. In the alumina refinery, precipitation tanks that operate within the particulate fouling field, but with an operating point close to the boundary with the crystallisation or erosion fields, may be amenable to small process changes that could stop particulate fouling from occurring. Although such process changes may decrease the specific gibbsite crystallisation rate, net productivity may increase as a result of greater tank availability. Conversely, if the operating point were far from a predominance boundary then increased tank availability may not be sufficient to offset the productivity decrease associated with reduced gibbsite crystallisation rate.

4. Conclusions

Scale formation in Bayer precipitation tanks occurs by crystallisation and/or particulate fouling. In particle free liquor, crystallisation fouling occurs; in slurry, crystallisation fouling, particulate fouling or erosion occurs. The key variables that determine the predominant fouling mechanism include: slurry solids loading, aluminate and/or oxalate supersaturation, and local slurry flow pattern and fluid velocity. The specific conditions under which one mode of fouling transitions to another may be mapped on so-called fouling predominance diagrams. Laboratory apparatus and procedures have been developed to measure scale formation under controlled conditions, thus allowing the fouling predominance diagrams to be produced over the range of conditions typical of Bayer precipitation tanks. This data will assist in optimising scale formation with respect to precipitation productivity.

5. Acknowledgements

This project was undertaken with financial support, and in kind equipment and personnel support from Queensland Alumina Limited; it forms part of a strategic initiative between The University of Queensland and Queensland Alumina Limited in the field of Bayer process research.

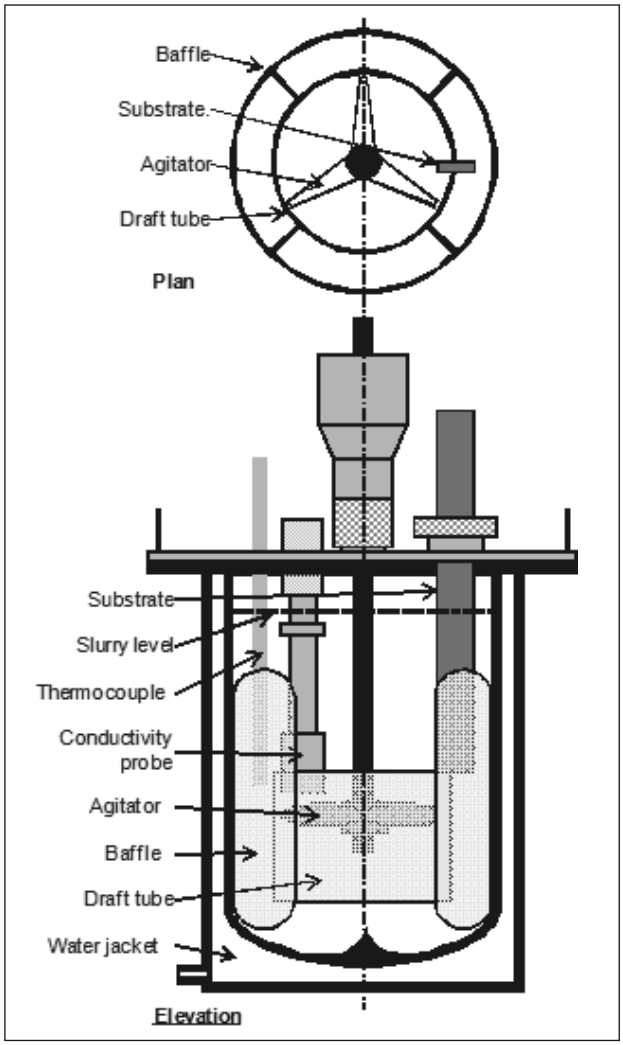

Figure 1. Schematic diagram of the laboratory stirred tank crystalliser

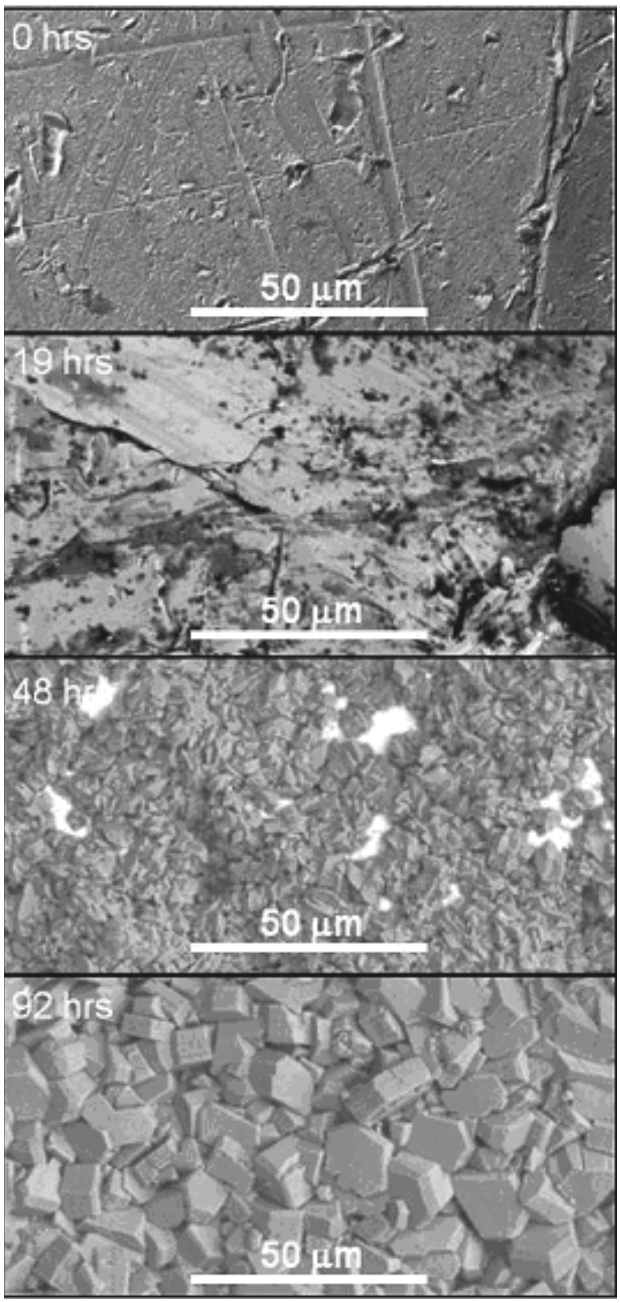

Figure 2. SEM images of crystallisation fouling of Gibbsite on roughened steel plate.

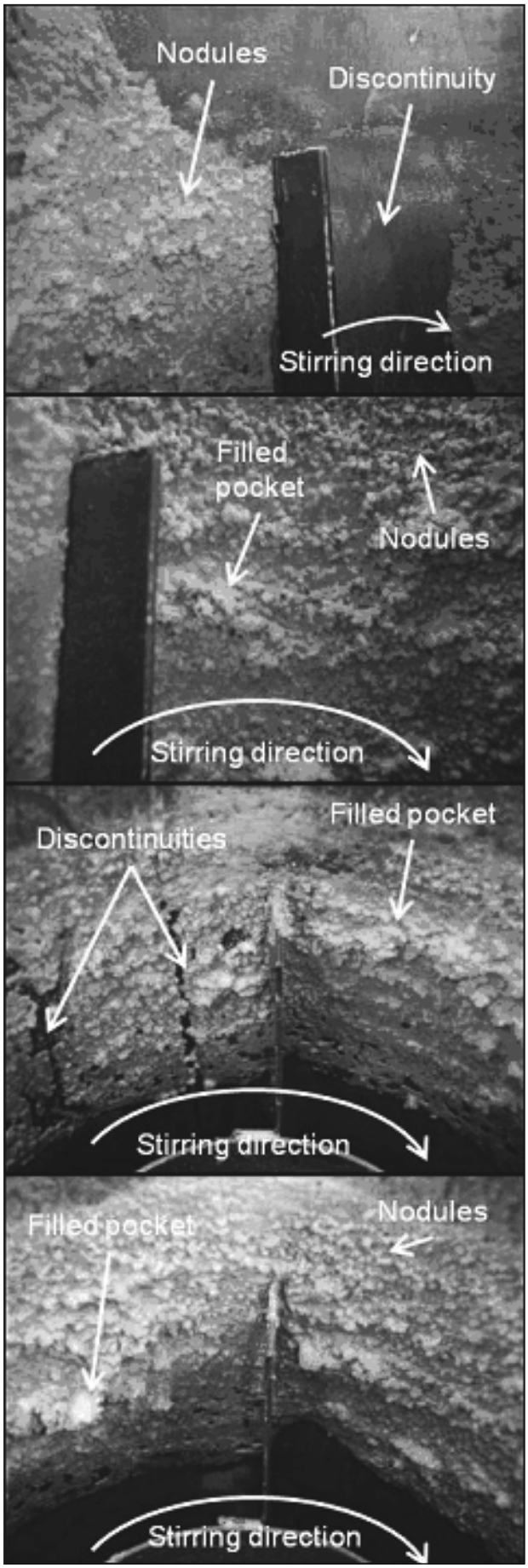

Figure 3. Scale formed in a stirred tank vessel after ~5 days (T = 65°C, s_g = 0.6, s_{ox} = 1.4, f = 2.1%, stirring = 300 rpm).

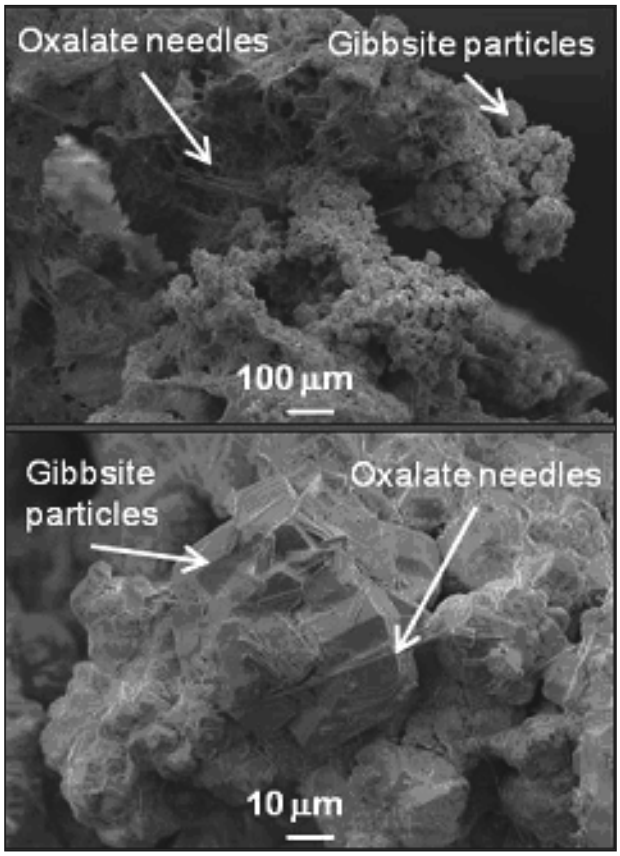

Figure 4. Gibbsite/oxalate particulate scale in a stirred vessel. T=65°C, s_g=0.6, s_{ox}=1.4, f= 2.1%, 300 rpm, 5 days.

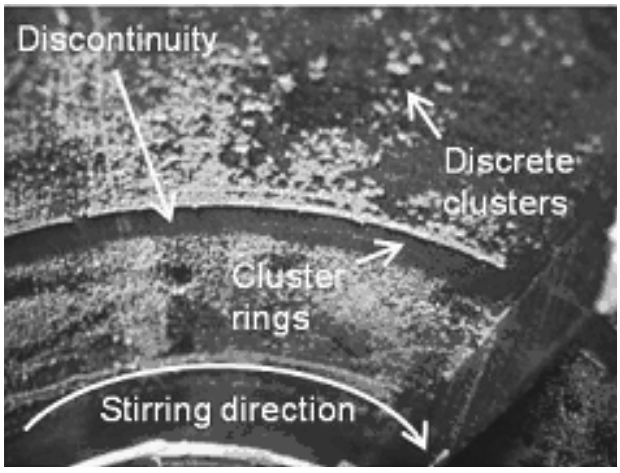

Figure 5. An example of oxalate particulate fouling in a stirred tank vessel.

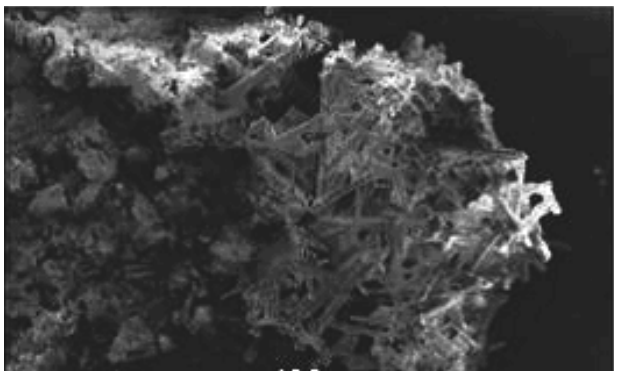

Figure 6. An example of oxalate particulate scale.

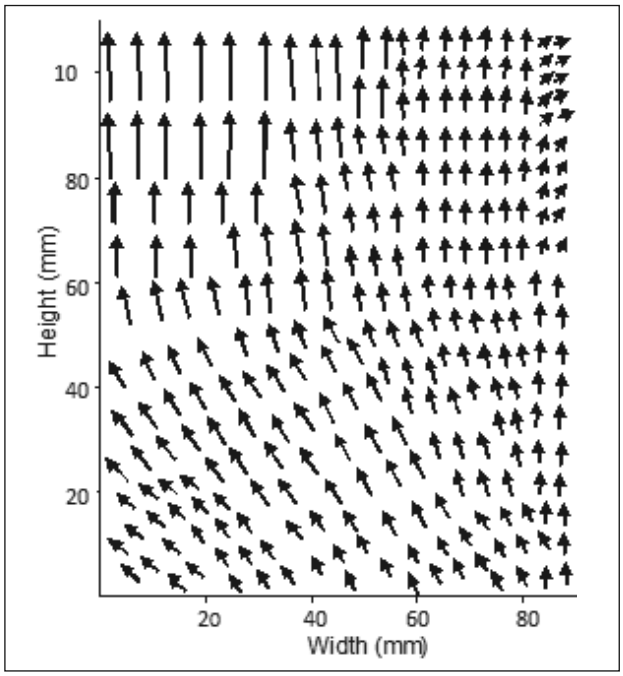

Figure 7. An example of the velocity profile in the model crystalliser

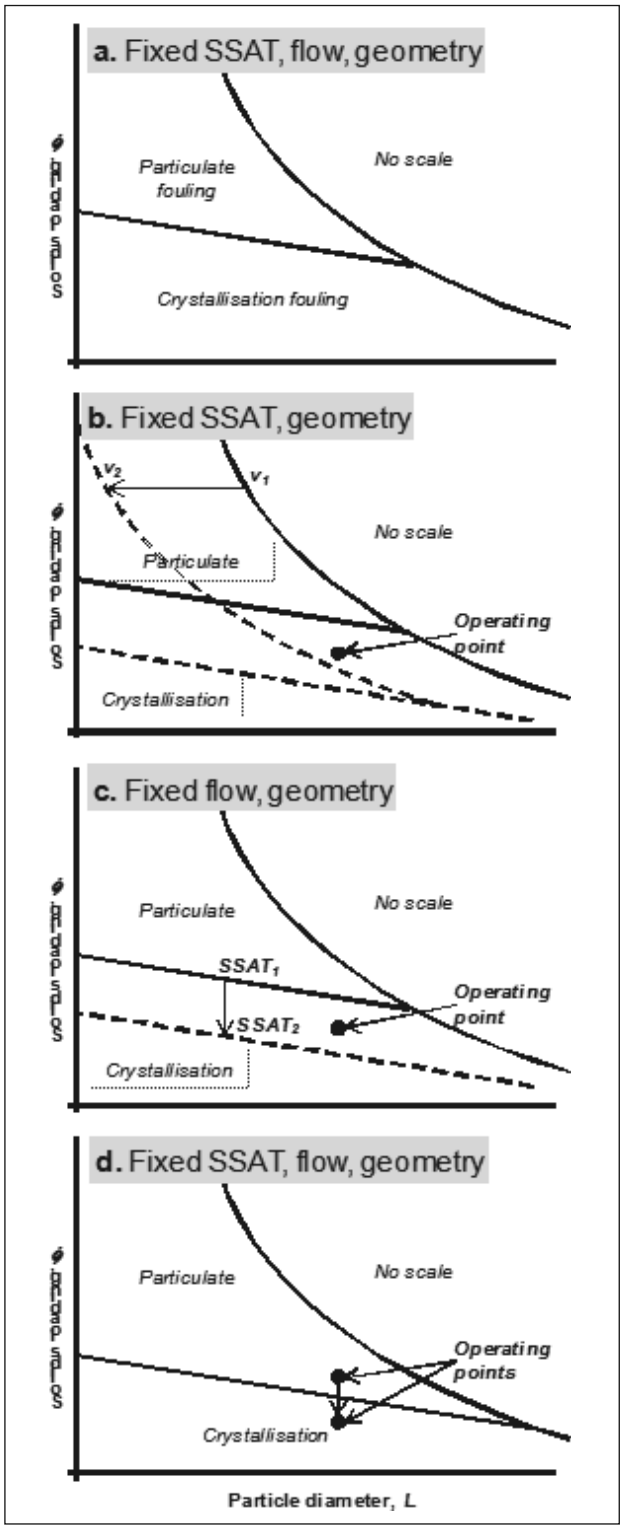

Figure 8. Hypothetical scaling predominance diagrams ($v_2 > v_1$, $SSAT_2 > SSAT_1$, $f_2 > f_1$).

References

Alumina Technology Roadmap, May 2006,: September 1, 2011, from http://www.world-aluminium.org/cache/fl0000227.pdf

Alumina Technology Roadmap, 2010 Update (8th draft), September 1, 2011, from http://www.world-aluminium.org/cache/fl0000422.pdf

Audet D., Rossiter D. and Sipos G., 2005, 'Evaluation of number based particle size analysers', in proceedings of: *7th Alumina Quality Workshop*, Perth, Australia, pp.174-177

Bott T, 1997, 'Aspects of crystallization fouling', *Experimental Thermal and Fluid Science,* vol.14, no. 4, pp.356-360.

Breault R. and Bouchard N., 2008, 'Electrochemical scale inhibition - how a cathodic current prevents scaling', in proceedings of: *8th Alumina Quality Workshop*, Darwin, Australia, pp.328-333.

Characklis W, and Marshal K., 1990, *Microbial Fouling*, Wiley, New York.

Connop W., 1996, 'A new procedure for the determination of alumina, caustic and carbonate in bayer liquors', in proceedings of: *4th International Alumina Quality Workshop*, Darwin, Australia, pp.321-330.

Deev A., Rasheed T., Welsh M., Khan M.,and Rasul M., 2009, 'Measurement of instantaneous flow velocities in a concentric reducer using particle image velocimetry: study of scale deposition', *Experimental Thermal and Fluid Science*, vol.33, no.6, pp.1003-1011.

Epstein N., 1983, 'Thinking about heat transfer fouling: a 5 x 5 matrix', *Heat Transfer Engineering,* vol.4, no.1, pp.43-56.

Kern D., and Seaton R., 1959, 'A theoretical analysis of thermal surface fouling', *British Chemical Engineering,* vol.5, pp.258-262.

Kuppan T., 2000, *Heat Exchanger Design Handbook*', Marcel Dekker AG, New York.

Loan M., Klauber C. and Vernon C., 2008, 'A fundamental study of gibbsite scale nucleation on mild steel', in proceedings of: *8th International Alumina Quality Workshop*, Darwin, Australia, pp.334-339.

Muller-Steinhagen H., 2011, 'Heat Transfer fouling: 50 years after the Kern Seaton model', Heat Transfer Engineering, vol.32, pp.1-13

Nawrath S., Khan M. and Welsh M., 2006, 'An experimental study of scale growth rate and flow velocity of a super-saturated caustic-aluminate solution', *International Journal of Mineral Processing,* vol.80, no.2-4, pp.116-125.

Papavergos P. and Hedley A., 1984, 'Particle deposition behaviour from turbulent flows', Chemical *Engineering Research and Design*, vol.62, pp.275-295.

Pearson N., Becker T., Gale J., Jones F. and Ogden M., 2008, 'Analytical techniques to improve the understanding of scale of adhesion fundamentals', in proceedings of: *8th International Alumina Quality Workshop*, Darwin, Australia, pp.31-36.

Rasheed T., 2005, 'Scale growth study in a concentric reducer: measurement of instantaneous velocity using particle image velocimetry', Thesis, Central Queensland University,

Rihan R. and Nesic S., 2006, 'Erosion-corrosion of mild steel in hot caustic. part I: NaOH solution', *Corrosion Science*, vol.48, no.9, pp.2633-2659.

Roach G., 1994, 'Bayer Process Scale - Growth and Prevention', *Jamaica Bauxite Institute Journal*, vol.12, pp.22-34.

Roach G. and Cornell J., 1985, 'Scaling in Bayer Plants', *Chemeca 85*, Perth, pp.217-222.

Roach G.,and Cornell J., 1996, 'Scaling in Bayer Refineries', *Chemeca 96*, Perth, pp.275-279.

Rosenberg S. and Healy S., 1996, 'A Thermodynamic Model for Gibbsite Solubility in Bayer Liquors' in proceedings of: *Fourth International Alumina Quality Workshop*, Darwin, Australia, pp.301-310.

Scadan R. and Laurila T., 2008, 'Scale inhibition and control: results of a five year field study into unique electrochemical techniques' in proceedings of: *8th International Alumina Quality Workshop*, Darwin, Australia, pp.61-63.

Sweegers C., Boerrigter R., Grimbergen R., Meekes H., Fleming S., Hiralal I. and Rijkeboer A., 2002, 'Morphology prediction of gibbsite crystals - an explanation for the lozenge-shaped growth morphology', *Journal of Physical Chemistry B,* vol.106, no.5, pp.1004-1012.

Sweegers C., de Coninck H., Meekes H., van Enckvort W., Hiralal I. and, Rijkeboer A, 2001, 'Morphology, evolution and other characteristics of gibbsite crystals grown from pure and impure aqueous sodium aluminate solutions', *Journal of Crystal Growth,* vol. 233, no.3, pp.567-582.

Taborek J., Aoki T., Ritter R., Palen J. and Knudsen J., 1972, 'Fouling: the major unresolved problem in heat transfer', *Chemical Engineering Progress,* vol.68, no.2, pp.59-66.

Watkinson A. and Wilson D., 1997, 'Chemical reaction fouling: A review', *Experimental Thermal and Fluid Science*, vol.14, no.4, pp.361-374.

Webster N., Madsen I., Loan M., Scarlett N., and Wallwork K., 2009, 'A flow cell for in-situ synchrotron x-ray diffraction studies of scale formation under Bayer processing conditions', *Review of Scientific Instruments*, vol.80, no.8, pp.084102-084102-5

Wu J.,Nairn D., Nguyen B., Farrow J.and Stegink D., 2011, 'Scale suppression using swirl flow technology', *Metallurgical Plant Design and Operating Strategies*, Perth, Australia, pp.515-526